Int. J. New. Chem., 2024, Vol. 11, Issue 4, pp. 393-413.

International Journal of New Chemistry

Published online 2024 in http://www.ijnc.ir/.

Open Access

Print ISSN: 2645-7236

Online ISSN: 2383-188x

Original Research Article

Determination of Hg (II) in Food Specimens by a Straightforward Potentiometric Sensor Utilizing 5,12-dihydroquinoxalino(2,3-b)quinoxaline as the Ionophore

Zohreh Rostami[1]*, Katayoon Ahangarbahani[1], Maedeh Shadpourian[2], Dorna Abdolkhani[3,*]

[1] Department of Chemical Engineering-Biotechnology, Science and Research Branch, Islamic Azad University, Tehran, Iran.

[2] Department of Food Science and Technology, Tehran Medical Science, Islamic Azad University, Tehran, Iran.

[3,*] Ph.D student of Food Sciences and Industries, Biotechnology Orientation, Islamic Azad University Yasouj Branch, Yasouj,Iran.

*Corresponding author email address: dornaabdolkhani6@gmail.com

Received: 2024-01-04 *Accepted: 2024-03-10* *Published: 2024-03-16*

ABSTRACT

The research aimed to fabricate a coated graphite membrane electrode for the potentiometric measurement of mercury (II) using 5,12-dihydroquinoxalino(2,3-b)quinoxaline (L) as the ionophore. Density functional theory computations were employed to investigate the interaction of L with 10 different cations, revealing that L exhibited the strongest interaction with Hg (II). The optimized membrane entailed of 30% PVC, 9% L, 2% NaTPB, and 59% nitrobenzene (NB) yielded the best Nernstian response. The designed electrode revealed a broead linearity domain in the concentration range of 1×10^{-8}-1×10^{-3} mol L^{-1} with a slope of 31.2±0.3 mV $decade^{-1}$ and a limit of detection (LOD) of 7.5×10^{-9} mol L^{-1}. Selectivity testing using the matched potential method showed no significant interference, affirming the sensor's selectivity. The electrode exhibited a rapid response time of 5 seconds and a lifespan of 4 months. Additionally, the potential response of the electrode remained unaffected by solution pH within the range of 3.0-8.0. The impact of organic solvents on the potential response was also evaluated, demonstrating that the sensor kept its Nernstian behavior in solutions with up to 20% non-aqueous content. In addition, the electrode was successfully utilized to determine Hg (II) in edible samples and employed as an indicator electrode in the potentiometric titration of Hg (II).

Keywords: Ion selective electrode, Potentiometry, Mercury, PVC membrane, Sensor, Quinoxaline

Introduction

Mercury toxicity and exposure are significant public health concerns [1]. Mercury is a naturally occurring element that exists in various forms, including elemental (or metallic) mercury, inorganic mercury compounds, and organic mercury compounds such as methylmercury [2]. The most common oxidation state of mercury is Hg^{2+}.Exposure to mercury can occur through inhalation of mercury vapors, ingestion of contaminated food or water, or through skin contact with mercury-containing products [3]. Mercury is known to have toxic effects on the nervous, digestive and immune systems, and on lungs, kidneys, skin, and eyes [3]. It is particularly harmful to developing fetuses and young children, as it can affect their developing nervous systems [4]. The symptoms of mercury poisoning can vary depending on the form of mercury, the dose, and the duration of exposure [5]. Acute exposure to high levels of mercury vapors can cause severe lung damage, while chronic exposure to lower levels of mercury can lead to symptoms such as tremors, emotional changes, insomnia, memory loss, neuromuscular changes, headaches, and cognitive and motor dysfunction [6]. Sources of mercury exposure include coal-fired power plants, waste incinerators, and certain industrial processes that release mercury into the air and water [7]. Additionally, mercury is commonly found in certain consumer products such as thermometers, fluorescent light bulbs, and some types of batteries [7]. Contaminated fish and seafood are also significant sources of mercury exposure, particularly for populations that rely heavily on seafood as a dietary staple [8]. Therefore, the determination of Hg^{2+} is of great importance. Various techniques are used to accurately measure the concentration of mercury ions in samples including atomic absorption spectroscopy (AAS) [9], inductively coupled plasma mass spectrometry (ICP-MS) [10], cold vapor atomic absorption spectroscopy (CVAAS) [11], and cold vapor atomic fluorescence spectroscopy (CVAFS) [12]. The aforementioned analytical methods have some limitations including complex and high cost instrumentations, being time-consuming and requiring sophisticated operators for implementing the pretreatments and analysis procedure [13]. On the other hand, ion selective electrodes (ISEs) are advantageous in analytical chemistry due to their high specificity, making them essential for selectively measuring particular ions in medical diagnostics, environmental monitoring, and other applications [14]. They are simple to use, require minimal sample preparation, have a wide measurement range, high sensitivity, and are cost-effective compared to alternative techniques, making them valuable tools for various analytical and diagnostic applications, including even fieldwork and point-of-

care testing [15]. 5,12-dihydroquinoxalino(2,3-b)quinoxaline (L) which its structure is given in Figure 1 is a potential ligand that can form complexes with metal cations due to the presence of various nitrogen atoms and also aromatic rings [16]. Therefore, in this research the complexation of L with different cations was investigated by density functional theory computations and the results showed it forms the most stable complex with Hg (II). Then, a coated graphite ion selective electrode on its basis was developed for the measurement of Hg (II). Then, the applicability of the designed sensor in the measurement of Hg (II) at edible real samples was scrutinized.

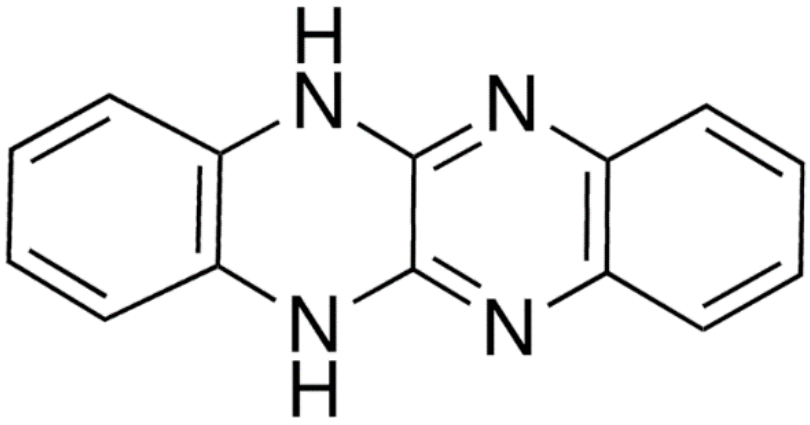

Fig. 1. The chemical structure of 5,12-dihydroquinoxalino(2,3-b)quinoxaline (L)

Materials and Methods

Computational Details

The L, M^{2+}, and their complexes structures were initially created using GuassView 6 [17]. Afterward, geometric optimization was carried out for each structure. Subsequently, the structures underwent computations for infrared (IR) using Gaussian 16 software [18] at the B3LYP/6-31G [d] level of theory with the density functional theory approach . For Cd^{2+}, Hg^{2+}, Pb^{2+}, and Ag^{+} ions, the LANL2DZ (Los Alamos National Laboratory of Double Zeta) basis set was utilized. These levels were selected based on previous research findings that were in line with experimental outcomes. The subsequent procedures were studied [19]:

$$L + Cation \rightarrow Complex \quad (1)$$

Eqs (2)–(6) were employed for the computation of adsorption energy values ($E_{Complexation}$) and thermodynamic parameters, encompassing the thermodynamic equilibrium constant ($\Delta S_{Complexation}$), Gibbs free energy changes ($\Delta G_{Complexation}$), and adsorption enthalpy changes ($\Delta H_{Complexation}$) [20].

$$E_{Complexation} = E_{Complex} - (E_{Cation} + E_L) \quad (2)$$

$$\Delta S_{Complexation} = S_{Complex} - (S_{Cation} + S_L) \quad (3)$$

$$\Delta G_{Complexation} = G_{Complex} - (G_{Cation} + G_L) \quad (4)$$

$$\Delta H_{Complexation} = H_{Complex} - (H_{Cation} + H_L) \quad (5)$$

In the preceding equations, E represents the total electronic energy for each structure, H stands for the evaluated materials' total energy plus the enthalpy's thermal correction. The G represents the total energy, plus the Gibbs free energy thermal correction, for each structure under investigation [21].

Apparatus and Chemicals

The pH measurements were conducted using two different instruments. Firstly, a Metrohm 827 pH meter equipped with a combined glass electrode was utilized for the measurements. Additionally, potential measurements at 25.0 ±0.1℃ were carried out using a 250 pH/mV meter Corning ion analyzer, with a saturated calomel electrode (SCE) serving as the reference electrode. The Ionophore (L) and all other chemicals and reagents utilized in the experiment were sourced from reputable suppliers such as Sigma-Aldrich or Merck (Darmstadt, Germany) without the need for additional purification. It is important to note that all solutions were prepared using double-distilled water (DDW) to ensure the accuracy and reliability of the results. Real samples, including three different marine salts, were sourced from a local supermarket in Tehran, Iran.

Electrode construction

The fabrication of electrodes involves several precise stages. Initially, specific quantities of Ionophore (L), polyvinyl chloride (PVC), sodium tetraphenylborate (NaTPB), nitrobenzene (NB), dioctyl phthalate (DOP), dibutyl phthalate (DBP), and oleic acid (OA) are carefully measured in a 5-ml beaker. Subsequently, the mixture is treated with 3 ml of tetrahydrofuran (THF) and subjected to ultrasonic treatment at low temperature to ensure thorough homogenization. Once the solution settles underneath a hood and becomes an oily and viscous mixture, a graphite bar is submerged to create a thin layer of polymer film. Following this, the film is allowed to dry at room temperature for 48 hours. To finalize the electrode preparation, it is immersed in a 1×10^{-3} mol L^{-1} $HgCl_2$ solution for 24 hours.

Real sample analysis

After dissolving 1g of marine salt in 500 ml of DDW, the solution was tested using a designed electrode to measure its potential response. The Hg (II) content of the solution was determined using a calibration curve. To verify the accuracy of the results, the samples were also analyzed using a standard spectrophotometric method. The spectrophotometric analytical procedure described involves the use of a calibrated flask to measure a solution containing a specific amount of Hg (II). The solution is then treated with sodium dodecyl sulfate (SDS), sulfuric acid, and dithizone, and diluted with double distilled water. The absorbance of the prepared standard solutions is measured at 490 nm, and a calibration curve is drawn [22]. This procedure is commonly used in analytical chemistry to determine the concentration of Hg (II) in a given sample [49]. Afterwards, the identical method was utilized on the actual samples to measure their Hg (II) concentrations, and the findings from both methods were assessed through statistical t-test analysis.

Experimental procedure

Once the membrane was prepared by blending 9mg of L, 2mg of an ionic additive, 59mg of NB, and 30mg of PVC, the subsequent procedure involved dissolving the ingredients in THF. After dissolution, the solution was allowed to sit at room temperature to allow the surplus THF to evaporate, leading to the formation of a thick, oily solution. Subsequently, the graphite bar was

immersed in the oily solution for about 5 seconds. After the electrode was inserted into the room to dry, it was then dipped in a 1×10-3 mol L-1 $HgCl_2$ solution for conditioning. This process helps to prepare the electrode for its analytical function. Following the conditioning phase, the electrode was linked to a potentiometer equipped with an Ag/AgCl reference electrode. The potentiometer assesses the electromotive force between the electrodes, functioning as the analytical signal. This signal demonstrates a direct association with the activity of Hg (II) as outlined by the Nernst equation (scheme 1). This procedure facilitates precise determination of Hg (II) activity, playing a crucial role in diverse analytical and scientific purposes.

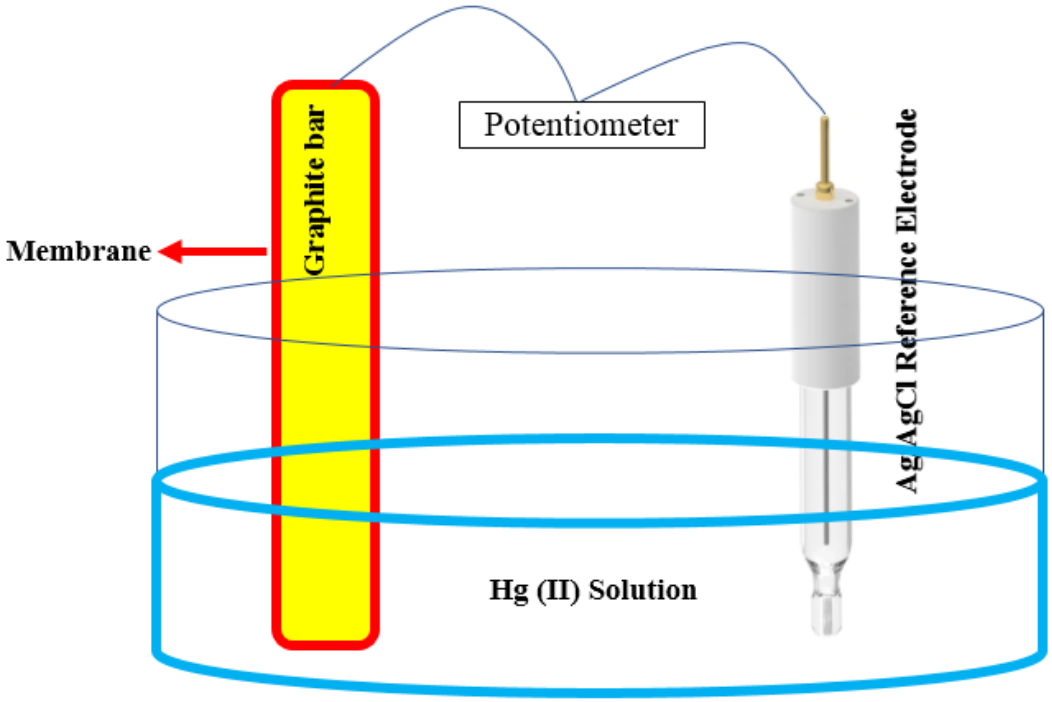

Scheme 1. The Hg (II) measurement process by the suggested sensor

Results and Discussion

Theoretical Results

Figure 2 depicts the initial structure of L complexes with metal cations, showing the incorporation of the metallic atom at the center of the molecular structure of L. The distance between the metal atom and the nitrogen heteroatoms is around 3Å, an arrangement critical for understanding coordination and bonding interactions. The results in Table 1 demonstrate that after undergoing geometrical optimizations, the complex structure was subjected to IR

computations. The computed complexation energies for all 10 scrutinized cations were found to be negative, indicating that the complexation of L with all cations is experimentally feasible [23]. This suggests that the complex formation between the ligand and cations is energetically favorable. The exothermic and spontaneous nature of the interaction between L and all cations is implied by the negative values of $\Delta H_{Complexation}$ and $\Delta G_{Complexation}$. Furthermore, the positive values of $\Delta S_{Complexation}$ indicate that the complexation process may not align with entropy favorability, potentially stemming from the aggregation following the complexation [24]. However, the most negative complexation energy, $\Delta H_{Complexation}$ and $\Delta G_{Complexation}$ were obtained for Hg (II) indicating L has a stronger interaction with this cation in comparison to others [25]. The optimized structure of the Hg^{2+}-L complex is depicted in Figure 3, revealing significant structural distortions resulting from geometrical optimizations. This observation suggests the presence of strong interactions within the complex. Consequently, Hg^{2+} was chosen as the primary analyte due to its high affinity for the ionophore.

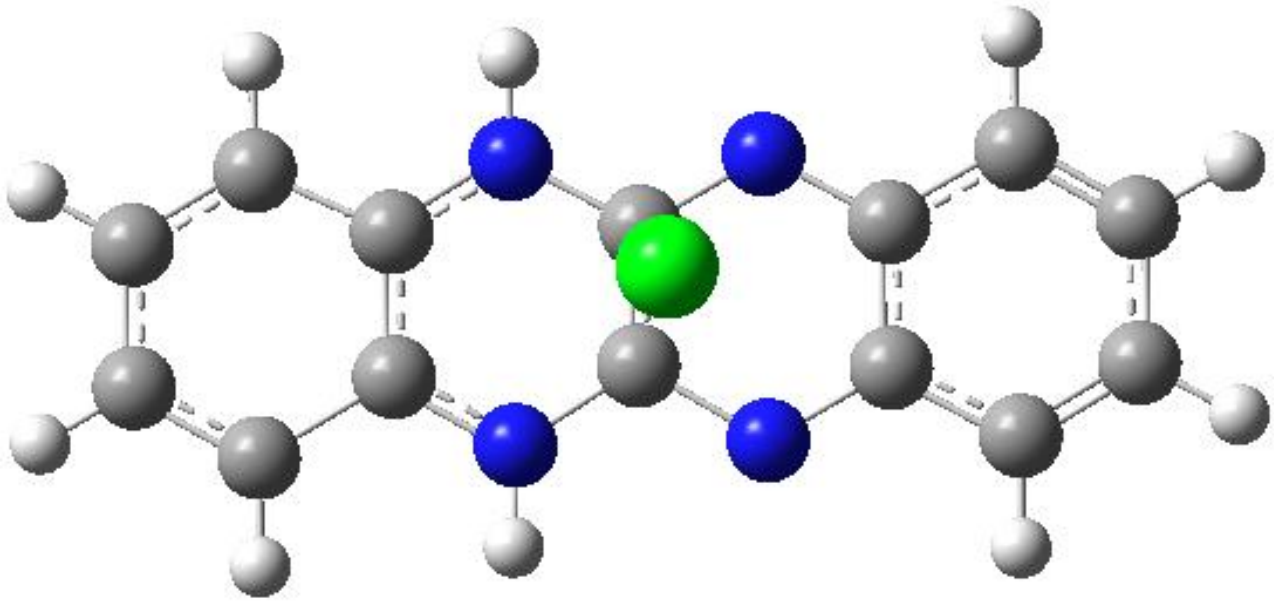

Fig. 2. The initial structure of L-Cation complex (gray: carbon, white: hydrogen, blue: nitrogen, green: metal cation atom)

Table 1. The calculated complexation energies and thermodynamic parameters

Complexes	$E_{Complexation}$ (kJ/mol)	$\Delta G_{Complexation}$ (kJ/mol)	$\Delta H_{Complexation}$ (kJ/mol)	$\Delta S_{Complexation}$ (J/mol)
Cu^{2+}-L	-154.361	-132.871	-80.420	-29.091
Zn^{2+}-L	-103.729	-70.502	-10.498	-41.030
Pb^{2+}-L	-80.281	-54.386	-6.719	-38.732
Mn^{2+}-L	-40.159	-10.342	-8.251	-25.981
Ag^{+}-L	-140.982	-110.568	-75.639	-22.345
Hg^{2+}-L	-180.230	-150.192	-90.498	-20.385
Fe^{3+}-L	-70.740	-43.837	-9.918	-30.498
Cd^{2+}-L	-20.493	-1.093	-0.487	-33.194
Cr^{3+}-L	-60.139	-33.874	-10.291	-40.984
Mg^{2+}-L	-19.109	-0.121	-0.678	-41.084

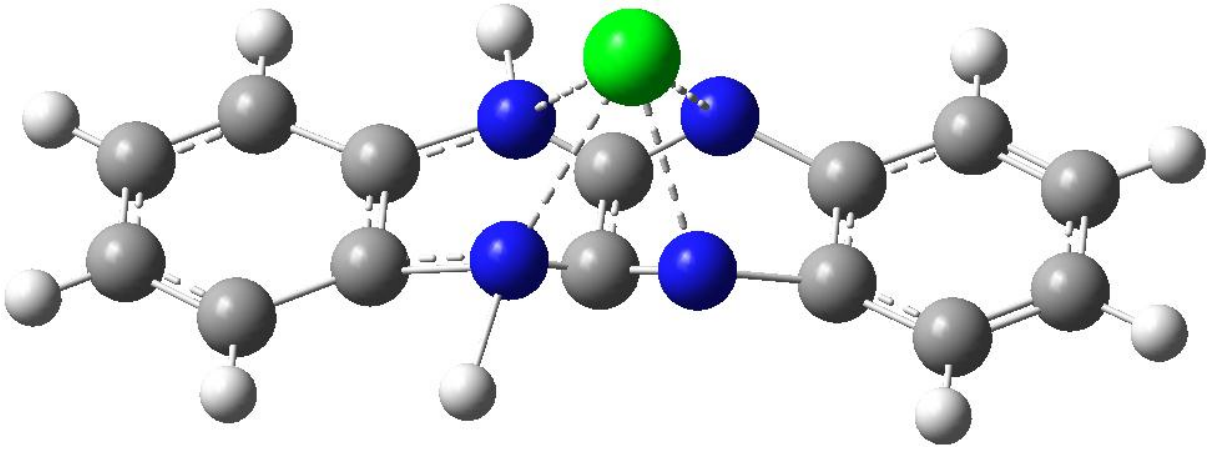

Fig 3. The optimized structure of Hg^{2+}-L Complex (gray: carbon, white: hydrogen, blue: nitrogen, green: Hg)

Optimization of membrane composition

For enhancing the efficacy of an ion selective electrode, it is vital to meticulously assess the composition of the membrane. Elements like the ionophore nature and amount, the plasticizer's dielectric constant, and the inclusion of ionic additives significantly influence the membrane's reactivity. Hence, comprehensive testing and evaluation of these membrane constituents are imperative to attain the targeted sensor performance. Therefore, when developing a new PVC-membrane ion-selective electrode, it is essential to begin by optimizing the membrane composition. This process may involve experimenting with different combinations of ionophores, plasticizers, and ionic additives to achieve the desired sensor performance. The research delved into investigating the potential reactions of 14 different electrodes of varied compositions, emphasizing the influence of ionophore quantity. Seven electrodes were constructed with varying ionophore amounts, and their performance was analyzed. The findings indicated that the selection of ionophore significantly impacted the sensors' potential reactions. In particular, the ionophore-free electrode (membrane 2) displayed a restricted linear range and a modest slope. This suggests that the absence of ionophore constrained the electrode's performance. However, as the ionophore amount was raised to 9% (membrane 7), the electrode exhibited a commendable Nernstian response with a slope of 26.2 mV/Decade. Moreover, this increase in ionophore content broadened the electrode's linear range, encompassing a wider dynamic range from 1.0×10^{-8} to 1.0×10^{-3}. These results underline the pivotal role of ionophore in influencing electrode potential reactions and overall performance. By showcasing the considerable impact of ionophore content on electrode behavior, the study offers valuable insights for refining sensor design and performance across various uses. This phenomenon implies that the ionophore has a strong interaction with Hg^{2+} [26]. These findings demonstrate the importance of carefully considering the amount of ionophore in electrode composition for optimal sensor performance. The results indicate that adding more ionophore can lead to membrane saturation, which in turn decreases the slope of the calibration curve for membrane 8. Additionally, it is crucial to consider the amount of ionic additive, as this can significantly impact sensitivity and the linear range. The findings highlight that using 2% NaTPB as the optimum amount can improve sensitivity and widen the linear range of the membrane [27]. The performance of the electrode is greatly influenced by the choice of plasticizer used, and through the exploration of different plasticizers, it was determined that NB resulted in the most favorable

outcome. The preference for NB as a plasticizer can be pertinent to its polar nature and high dielectric constant, which have the potential to improve the interaction between the analyte and the plasticizer [28]. This discovery holds particular significance for applications involving Hg (II) as a bivalent cation. The calibration curve of membrane 13, which exhibited the most optimal response, is presented in Fig. 4. This finding suggests that NB has unique properties that make it well-suited for enhancing the performance of membranes in analytical applications, especially when dealing with specific bivalent cations such as Hg (II). The polar nature of NB allows for strong interactions with the analyte, while its high dielectric constant further enhances these interactions, leading to improved sensitivity and selectivity in analytical measurements [29]. These characteristics make NB a promising candidate for use in membrane-based analytical techniques, where the interaction between the analyte and the membrane material plays a crucial role in determining the overall performance of the analytical system.

Table 2. Optimizing membrane composition

No	PVC (%wt)	Ionophore (%wt)	NaTPB (%wt)	Plasticizer (%59)	Linear Range (mol L^{-1})	Slope (mV/Decade)	LOD (mol L^{-1})
1	41	0	0	DBP	1.0×10^{-4} to 1.0×10^{-3}	8.9±0.2	9.5×10^{-5}
2	39	0	2	DBP	1.0×10^{-4} to 1.0×10^{-3}	10.9±0.3	9.0×10^{-5}
3	38	1	2	DBP	1.0×10^{-5} to 1.0×10^{-3}	14.8±0.2	9.5×10^{-6}
4	36	3	2	DBP	1.0×10^{-5} to 1.0×10^{-3}	16.7±0.1	9.0×10^{-6}
5	34	5	2	DBP	1.0×10^{-5} to 1.0×10^{-3}	19.9±0.3	8.0×10^{-6}
6	32	7	2	DBP	6.0×10^{-8} to 1.0×10^{-3}	22.1±0.2	5.5×10^{-8}
7	30	9	2	DBP	1.0×10^{-8} to 1.0×10^{-3}	26.2±0.2	9.0×10^{-9}
8	29	10	2	DBP	5.0×10^{-8} to 1.0×10^{-3}	24.2±0.2	3.0×10^{-8}
9	32	9	0	DBP	5.0×10^{-8} to 1.0×10^{-3}	20.8±0.1	4.0×10^{-8}
10	33	9	1	DBP	3.0×10^{-8} to 1.0×10^{-3}	22.5±0.3	1.5×10^{-8}
11	29	9	3	DBP	1.0×10^{-8} to 1.0×10^{-3}	25.3±0.2	9.0×10^{-9}
12	30	9	2	OA	3.0×10^{-8} to 1.0×10^{-3}	27.3±0.1	1.0×10^{-8}
13	30	9	2	NB	1.0×10^{-8} to 1.0×10^{-3}	31.2±0.3	7.5×10^{-9}
14	30	9	2	DOP	5.0×10^{-8} to 1.0×10^{-3}	25.9±0.2	1.0×10^{-8}

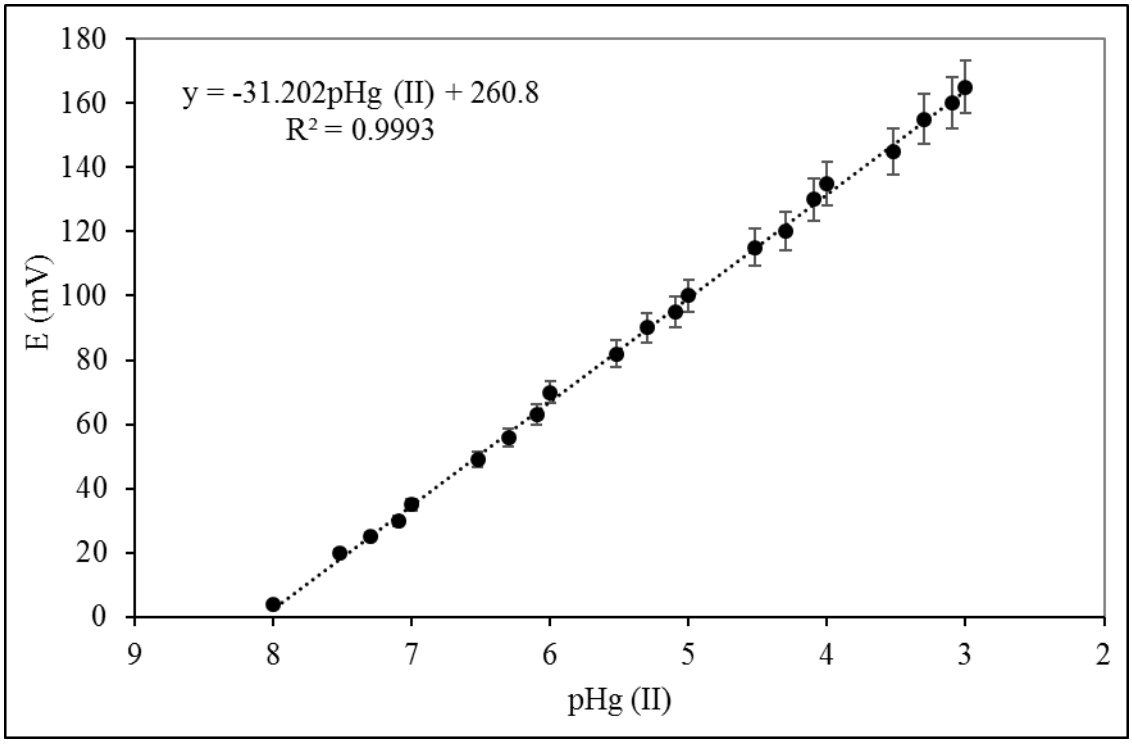

Fig. 4. The obtained calibration curve from membrane 13

Response time, lifespan, repeatability, and reproducibility

The accurate detection and measurement of ion concentrations using potentiometric sensing systems is greatly influenced by the response time, which is determined by the speed of complexation-decomplexation kinetics of analyte ions when an ionophore is present at the membrane surface [30]. The study involved submerging the reference and indicator electrodes in Hg (II) solutions with activities varying by a factor of 10. The sensor's performance was evaluated by continuously recording the electromotive force. The results indicated a quick 5-second response time for accurately measuring Hg (II) activity. Furthermore, the research assessed the endurance of the electrode by monitoring their performance over a 20-week period. This was done to ascertain their consistency in delivering dependable measurements. The swift response time demonstrates its ability for real-time measurements, and the prolonged monitoring period underscored the electrodes' reliability. The sensor exhibited a steady incline over a span of 16 weeks, illustrated in Fig. 6, indicating consistent Nernstian behavior without any deviations. This behavior can be attributed to the restricted solubility of L in inorganic solvents and its

outstanding chemical stability. Nevertheless, during the 17th week, there was an uptick in the sensor's limit of detection (LOD) to 5.0×10^{-8}, leading to a narrower linear range [31]. To evaluate the consistency of the designed potentiometric sensor, we prepared five Hg^{2+} solutions with activities of 1.0×10^{-7} and 1.0×10^{-5} and measured their potential responses. The resulting RSD% values of 3.82% and 2.33% indicate the sensor's precision in measuring different Hg^{2+} concentrations. Lower RSD% values reflect higher repeatability, showcasing the sensor's ability to consistently yield dependable results. To investigate the reproducibility, five electrodes were utilized to evaluate the potential response of two Hg^{2+} solutions with varying activity levels. The RSD% values of 5.12% and 4.08% indicate reliable precision and consistency in determining the potential response of Hg^{2+} solutions.

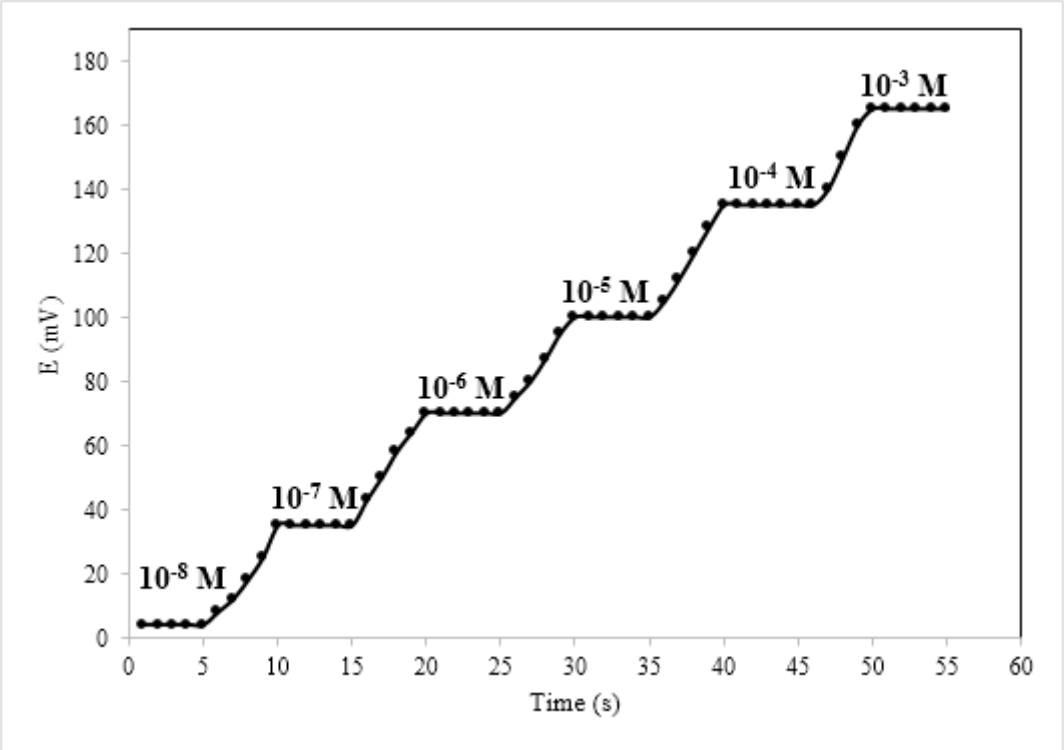

Fig. 5. The dynamic response time of the suggested electrode

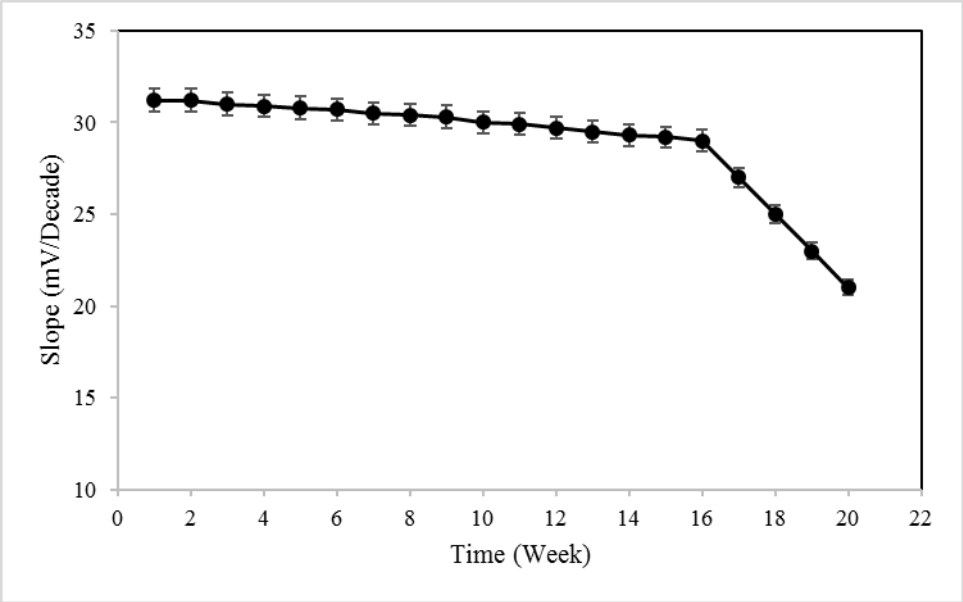

Fig. 6. The lifespan of the suggested potentiometric sensor

Applicable pH range

Nernstian behavior is crucial for the functionality of ion-selective electrodes, as it allows for accurate measurement of ion concentrations. However, this behavior could only be witnessed within a specific pH range. Hence, it is essential to investigate and determine the applicable pH scope in order to develop reliable and effective ion-selective electrodes. Understanding the pH range in which Nernstian behavior occurs will ensure that the electrodes can provide accurate and precise measurements across a variety of samples and conditions. During the experiment, a meticulously prepared 1.0×10^{-6} Hg^{2+} solution was subjected to pH testing ranging from 1.0 to 12.0 using concentrated solutions of sodium hydroxide and hydrochloric acid. The resulting potential measurements were recorded and charted against the corresponding pH values to investigate the correlation. The objective was to gain insight into how the Hg^{2+} solution behaves under varying pH conditions and to generate dependable data for comprehending its response to pH fluctuations. The data revealed that the sensor's response was consistent and independent within the pH range of 3.0 to 8.0. This suggests that the sensor is effective in detecting Hg^{2+} ions within this specific pH range. In acidic conditions with pH values below 3.0, the ionophore undergoes protonation, resulting in a complex interplay between hydronium ions and the analyte for binding with the ionophore [32]. This phenomenon introduces a competitive dynamic where both hydronium ions and the analyte vie for complex formation with the ionophore. The

protonation of the ionophore at such low pH levels significantly impacts the equilibrium of complex formation, thereby influencing the overall analytical process. Conversely, in alkaline environments with a pH exceeding 8.0, the cation forms complexes with hydroxyl ions [33]. As a result, it was determined that the effective functionality of the created ion-selective electrode is only guaranteed within a specific pH range of 3.0-8.0.

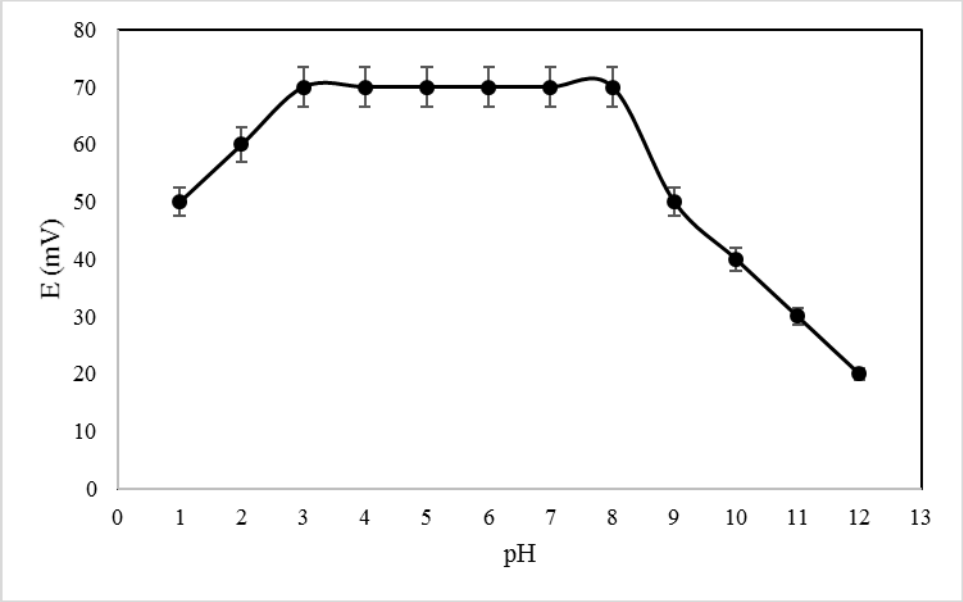

Fig. 7. The influence of pH on the potential response of the suggested sensor in a 1×10^{-6} mol L^{-1} solution of Hg (II) at ambient temperature

Selectivity

The assessment of the designed sensor's selectivity involved the application of the matched potential method (MPM) [34] using 16 different ionic species. Subsequently, the selectivity coefficients (K_{MPM}) were determined to gauge the sensor's responsiveness to various ions. The K_{MPM} values obtained from Table 3 offer valuable insights into the sensor's ability to differentiate between the analyte and interfering ions. A K_{MPM} value approaching 1 signifies a comparable potential response to both the analyte and interfering ion, while a value close to 0 indicates a minimal affinity towards the interfering ion. Upon examination of Table 3, it is clear that all selectivity coefficients are significantly smaller than 1 by 100-10000 folds, indicating remarkable selectivity of the developed sensor for Hg^{2+}. This validates the sensor's capability to

specifically identify Hg^{2+} in the presence of various other ionic species, showcasing its potential for practical applications where selectivity is essential

Table 3. The K_{MPM} Values

Ion	K_{MPM}	Ion	K_{MPM}
Ca^{2+}	4.1×10^{-4}	Al^{3+}	1.5×10^{-4}
Mn^{2+}	3.1×10^{-4}	Co^{2+}	3.7×10^{-3}
Mg^{2+}	2.6×10^{-3}	Se^{4+}	2.1×10^{-4}
Fe^{2+}	1.1×10^{-3}	Cu^{2+}	2.2×10^{-2}
Fe^{3+}	9.9×10^{-3}	K^{+}	2.6×10^{-3}
Ag^{+}	1.1×10^{-2}	Na^{+}	1.6×10^{-3}
Pb^{2+}	2.1×10^{-2}	Ni^{2+}	7.1×10^{-3}
Cd^{2+}	4.5×10^{-3}	Zn^{2+}	6.5×10^{-3}

The influence of partially non-aqueous mediums on potential response of the electrode

In order to evaluate the functionality of the suggested sensor in partially non-aqueous environments, it is necessary to carry out tests using different proportions of organic solvents. In this research, three sets of Hg^{2+} solutions were formulated with varying levels of ethanol, acetone, and a mix of both. The objective was to examine the performance of the sensor when exposed to these organic solvents, a critical factor for its possible use in analyzing authentic samples containing such compounds. The findings presented in Table 4 illustrate that the newly developed electrode maintains its sensitivity and linear range even when subjected to solutions with a 20% organic content. However, it was observed that with the introduction of additional organic components, there was a reduction in the slope and an increase in the limit of detection (LOD). This phenomenon is likely attributable to the potential seepage of ionophore and other membrane constituents into the test solution when it contains elevated levels of organic solvents [33].

Table 4. The proposed sensor function in non-aqueous mediums

Non aqueous content (%v/v)	Slope (mV.Decade^{-1})	Dynamic Range (mol L^{-1})
0	31.2±0.3	1.0×10^{-8} to 1.0×10^{-3}
Ethanol		
5	31.1±0.3	1.0×10^{-8} to 1.0×10^{-3}
10	29.9±0.4	1.0×10^{-8} to 1.0×10^{-3}
15	29.5±0.3	1.0×10^{-8} to 1.0×10^{-3}
20	28.8±0.2	1.0×10^{-8} to 1.0×10^{-3}
25	23.1±0.2	1.0×10^{-7} to 1.0×10^{-3}
Acetone		
5	31.2±0.2	1.0×10^{-8} to 1.0×10^{-3}
10	31.0±0.4	1.0×10^{-8} to 1.0×10^{-3}
15	29.1±0.2	1.0×10^{-8} to 1.0×10^{-3}
20	28.5±0.3	1.0×10^{-8} to 1.0×10^{-3}
25	22.8.3±0.6	1.0×10^{-7} to 1.0×10^{-3}
Combination of 1:1 (Ethanol:Acetone)		
5	31.0±0.4	1.0×10^{-8} to 1.0×10^{-3}
10	29.7±0.2	1.0×10^{-8} to 1.0×10^{-3}
15	28.2±0.2	1.0×10^{-8} to 1.0×10^{-3}
20	27.1±0.5	1.0×10^{-8} to 1.0×10^{-3}
25	20.8±0.3	1.0×10^{-7} to 1.0×10^{-3}

Analytical applications

The electrode designed for analyzing Hg^{2+} levels in marine salts was successfully used to test 3 different samples, with the results presented in Table 5. The samples were also analyzed using a standard spectrophotometric method, and the results from both techniques were compared using a t-test. The calculated experimental t values were consistently lower than the critical t values, indicating good agreement between the results of both methods. In addition to this, the

applicability of the proposed electrode in indirect potentiometry was examined by titrating a 20 ml solution of 1×10^{-6} mol L^{-1} Hg^{2+} with a 1×10^{-4} mol L^{-1} solution of EDTA (Ethylenediaminetetraacetic acid). The resulting titration curve, shown in Figure 6, clearly indicates the easily observable equivalent point at 200 µL.

Table 5. Analysis of Hg^{2+}in marine salt samples (n=3)

Sample	Measured by the developed electrode (µM)	Measured by spectrophotometric method (µM)	Calculated experimental T	Critical T (at 95% confidence level and 4 degree of freedom)
Marine Salt 1	19.8±0.7[a]	18.6±0.8	1.92	2.78
Marine Salt 2	39.1±1.0	40.9±0.9	2.34	2.78
Marine Salt 3	5.1±0.4	5.8±0.3	2.38	2.78

[a] Standard deviation based on three replicates

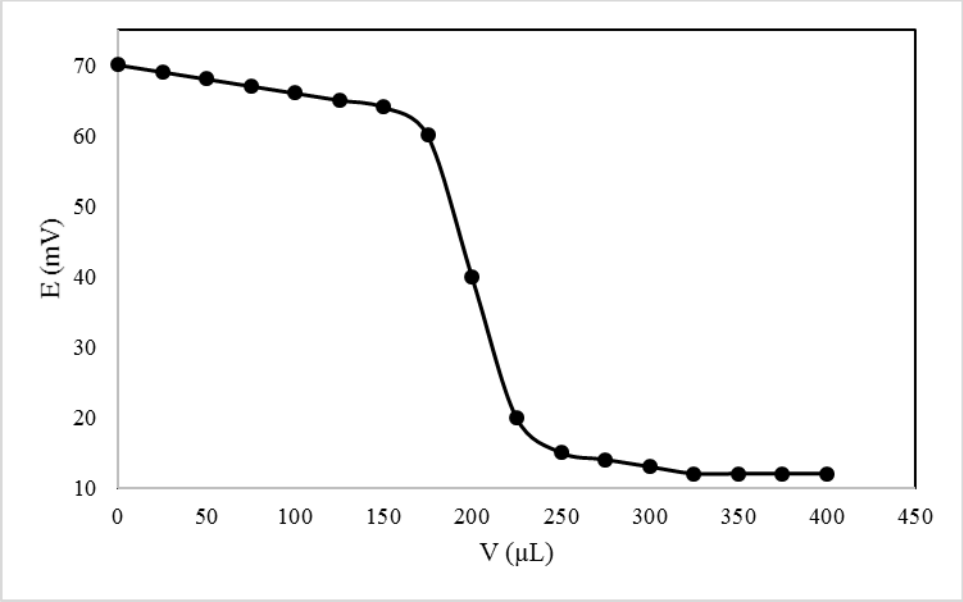

Figure 6. Titration curve of a 1×10^{-6} mol L^{-1} solution of Hg^{2+} with a 1×10^{-4} mol L^{-1} solution of EDTA

Comparison with best former reports

Table 6 compares the key analytical figures of merit of the suggested electrode in this research with some of the best former reported electrodes. The proposed electrode demonstrates the

highest Nernstian slope, the lowest detection limit, and the shortest response time among the compared electrodes. These results indicate that the suggested sensor in this paper outperforms the former ones.

Table 6. Comparison of the analytical figures of merit of the proposed electrode with some of the best previously reported ones

Linear range (M)	LOD (M)	Slope (mV.Decade^{-1})	Response time (S)	pH range	Reference
1×10^{-7}-1×10^{-1}	7.0×10^{-8}	28.0	6	2.5-10	[35]
1×10^{-7}-1×10^{-1}	1.0×10^{-7}	28.1	15	1.5-3.5	[36]
1×10^{-6}-1×10^{-1}	3.0×10^{-8}	28.4	25	3.0-5.0	[37]
1×10^{-7}-1×10^{-2}	8.0×10^{-8}	29.7	15	1.7-4.0	[38]
1×10^{-6}-1×10^{-2}	7.9×10^{-7}	27.6	10	4.0-4.5	[39]
1×10^{-6}-1×10^{-2}	1.0×10^{-6}	27.8	20	1.0-6.0	[40]
1×10^{-8}-1×10^{-3}	**7.5×10^{-9}**	**31.2**	**5**	**3.0-8.0**	**This work**

Conclusion

The research focused on developing a PVC membrane electrode coated with graphite to potentiometrically measure mercury levels using 5,12-dihydroquinoxalino(2,3-b)quinoxaline (L) as the ionophore. Leveraging density functional theory computations, the team examined the interaction of L with 10 different cations and identified Hg (II) as exhibiting the strongest affinity with L. The best composition identified includes 30% PVC, 9% L, 2% NaTPB, and 59% nitrobenzene as the plasticizer, resulting in the most effective Nernstian response. The sensor's performance was characterized by a broad linearity in the concentration range of 1×10^{-8}-1×10^{-3} mol L^{-1}, with a slope of 31.2±0.3 mV decade-1 and a limit of detection (LOD) of 7.5×10^{-9} mol L^{-1}. The matched potential method was used to conduct selectivity testing, which confirmed that the sensor does not experience significant interference. Additionally, the electrode demonstrated

a rapid response time of 5 seconds and a long lifespan of 16 weeks. Furthermore, the potential response of the electrode remained consistent regardless of the solution pH, within the range of 3.0-8.0. The sensor's ability to maintain Nernstian behavior in solutions with up to 20% non-aqueous content demonstrates its robustness in various solvent environments. This finding is significant as it indicates the sensor's potential applicability in a wide range of industrial and environmental settings where organic solvents are commonly used. Furthermore, the successful measurement of Hg (II) levels in edible samples highlights the sensor's practical utility in food safety and quality control. Its use as an indicator electrode in the potentiometric titration of Hg (II) further underscores its versatility in analytical chemistry applications. Overall, these results suggest that the sensor holds promise for diverse uses, from environmental monitoring to food analysis and beyond.

References

1. A. Carocci, R. Nicola, M. S. Sinicropi, and G. Giuseppe, Rev. Environ. Contam. Toxicol., 2014 (2014) 1.
2. V. Branco, S. Caito, M. Farina, J. T. Rocha, M. Aschner, and C. Carvalho. J. Toxicol. Environ. Health., B. 20, (2017) 119.
3. M. C. Houston, J. Clin. Hypertens. 13(2011) 621.
4. V. Andreoli, F. Sprovieri, *Int. J. Environ*. Res. Public Health. 14(2017) 93.
5. N. J. Langford, R. E. Ferner, J. Hum. Hypertens. 13(1999) 651.
6. K. M. Rice, E. M. Walker Jr, M. Wu, C. Gillette, E. R. Blough, J. Prev. Med. Public. Health., 47(2014) 74.
7. L. Magos, T. W. Clarkson, Ann. Clin. Biochem., 43(2006) 257.
8. L. Yang, Y. Zhang, F. Wang, Z. Luo, S. Guo, U. Strähle, Chemosphere. 245 (2020) 125586.
9. L. N. Suvarapu, Y. K. Seo, S. O. Baek, Rev. Anal. Chem., 32(2013) 225.
10. L. Jian, W. Goessler, K. J. Irgolic, J. Anal. Chem. 366 (2000) 48.
11. H. Pyta, W. Rogula-Kozłowska, Microchem. J. 124 (2016) 76.
12. W. Geng, T. Nakajima, H. Takanashi, A. Ohki, J. Hazard. Mater. 154(2008) 325.
13. Y. Shao, Y. Ying, J. Ping, Chem. Soc. Rev. 49(2020) 4405.
14. C. R. Rousseau, P. Bühlmann, TrAC. Trends. Anal. Chem. 140 (2021) 116277.

15. Y. H. Cheong, L. Ge, G. Lisak, Anal. Chim. Acta., 1162 (2021) 338304.
16. A. M. Ashrafi, Z. Koudelkova, E. Sedlackova, L. Richtera, V. Adam, J. Electrochem. Soc., 165 (2018) B824.
17. Gaussian 16, Revision C.01, M. J. Frisch, G. W. Trucks, H. B. Schlegel, G. E. Scuseria, M. A. Robb, J. R. Cheeseman, G. Scalmani, V. Barone, G. A. Petersson, H. Nakatsuji, X. Li, M. Caricato, A. V. Marenich, J. Bloino, B. G. Janesko, R. Gomperts, B. Mennucci, H. P. Hratchian, J. V. Ortiz, A. F. Izmaylov, J. L. Sonnenberg, D. Williams-Young, F. Ding, F. Lipparini, F. Egidi, J. Goings, B. Peng, A. Petrone, T. Henderson, D. Ranasinghe, V. G. Zakrzewski, J. Gao, N. Rega, G. Zheng, W. Liang, M. Hada, M. Ehara, K. Toyota, R. Fukuda, J. Hasegawa, M. Ishida, T. Nakajima, Y. Honda, O. Kitao, H. Nakai, T. Vreven, K. Throssell, J. A. Montgomery, Jr., J. E. Peralta, F. Ogliaro, M. J. Bearpark, J. J. Heyd, E. N. Brothers, K. N. Kudin, V. N. Staroverov, T. A. Keith, R. Kobayashi, J. Normand, K. Raghavachari, A. P. Rendell, J. C. Burant, S. S. Iyengar, J. Tomasi, M. Cossi, J. M. Millam, M. Klene, C. Adamo, R. Cammi, J. W. Ochterski, R. L. Martin, K. Morokuma, O. Farkas, J. B. Foresman, and D. J. Fox, Gaussian, Inc., Wallingford CT, 2016.
18. GaussView, Version 6.1, Roy Dennington, Todd A. Keith, and John M. Millam, Semichem Inc., Shawnee Mission, KS, 2016.
19. B. Hassani, M. Karimian, N. Ghoreishi Amin, *Int. J. New. Chem.*, 11(2024): 204.
20. S. Tayebi-Moghaddam, P. Niknam Rad, M. Kohansal, *Int. J. New. Chem.*, 11(2024): 216.
21. S. Tayebi-Moghaddam, M. Aliakbari, K. Tayeboun, *Int. J. New. Chem.*, 11(2024) 82.
22. H. Khan, M. J. Ahmed, M. I. Bhanger, Anal. Sci. 21 (2005) 507.
23. M. R. Jalali Sarvestani, T. Madrakian, A. Afkhami, B. Ajdari, Microchem. J., 188 (2023) 108483.
24. M. R. Jalali Sarvestani, L. Hajiaghababaei, J. Najafpour, S. Suzangarzadeh, Anal. Bioanal. Electrochem., 10 (2018) 675.
25. A. Panahi Sarmad, L. Hajiaghababaei, A. S. Shahvelayati, J. Najafpour, Russ. J. Electrochem., 57 (2021) 774.
26. O. Isildak, I. Yildiz, R. Erenler, B. Dag, I. Isildak, B. Chem. Soc. JPN., 95(2022) 353.
27. A. Elgamouz, I. Shehadi, A. Assal, A. Bihi, A. N. Kawde, J. Electroanal. Chem. 895 (2021)115443.
28. N. Al Hakawati, S. S. Alharthi, A. F. de Namor, Arab. J. Chem. 13(2020) 8671.

29. M. Ghaemi, L. Hajiaghababaei, R. M. Tehrani, J. Najafpour, and A. S. Shahvelayati, *J. Mol. Liq.*, *370* (2023) 121043.
30. S. S. Alharthi, A. M. Fallatah, H. M. Al-Saidi, Sensors., 21 (2021) 3020.
31. H. R. Rashvand, L. Hajiaghababaei, M. R. Darvich, M. R. Jalali Sarvestani, F. J. Miyandoab, J. Anal. Chem. 75 (2020) 1340.
32. P. Khalatbarimohseni, M. R. Jalali Sarvestani, S. Ahmadi, M. Mahboubi-Rabbani, *Anal. Bioanal. Chem. Res.*, 11(2024) 169.
33. M. R. Jalali Sarvestani, R. Ahmadi, *Anal. Bioanal. Chem. Res.*, 5 (2018) 273.
34. V. P. Gadzekpo, G. D. Christian, Anal. Chim. Acta. 164 (1984) 279.
35. S. Kaushal, R. Badru, S. Kumar, S. K. Mittal, P. Singh, RSC Adv. 6(2016) 3150.
36. M. Naushad, T. A. Rangreez, Z. A. ALOthman, J. Electroanal. Chem. 713 (2014)125.
37. F. Bakhtiarzadeh, S. Ab Ghani, Electroanalysis., 22 (2010) 549.
38. S. M. Kermani, M. Ghanei-Motlagh, R. Zhiani, M. A. Taher, M. Fayazi, I. Razavipanah, J. Mol. Liq. 206 (2015) 145.
39. B. Dalkıran, A. D. Özel, S. Parlayan, E. Canel, U. Ocak, E. Kılıç, Monatsh Chem., 141 (2010) 829.
40. I. I. Abbas, Int. J. Chem. 4 (2012) 23.

HOW TO CITE THIS ARTICLE

Zohreh Rostami, Katayoon Ahangarbahani, Maedeh Shadpourian, Dorna Abdolkhani, "**Determination of Hg (II) in Food Specimens by a Straightforward Potentiometric Sensor Utilizing 5,12-dihydroquinoxalino(2,3-b)quinoxaline as the Ionophore**" International Journal of New Chemistry., 2024; 11(4), 393-413. DOI: https://doi.org/10.22034/ijnc.2024.711993